Available online at www.sciencedirect.com

SCIENCE DIRECT®

Electrochimica Acta 49 (2004) 3947–3955

ELECTROCHIMICA Acta

www.elsevier.com/locate/electacta

Formability of organic coatings—an electrochemical approach

A.C. Bastos[a], C. Ostwald[b], L. Engl[b], G. Grundmeier[c], A.M. Simões[a,*]

[a] DEQ, Instituto Superior Técnico, Av. Rovisco Pais, 1049-001 Lisboa, Portugal
[b] DOC Dortmunder Oberflachen Centrum, Eberhardstr. 12, 44145 Dortmund, Germany
[c] Max-Planck-Institut fur Eisenforschung, Max-Planck-Str. 1, 40237 Dusseldorf, Germany

Received 22 November 2003; received in revised form 17 March 2004; accepted 21 March 2004

Abstract

Coil-coated samples of electrogalvanised steel were submitted to uniaxial, biaxial and plane strain of various magnitudes and tested by electrochemical impedance spectroscopy (EIS). A good correlation was encountered between the coating resistance and the equivalent plastic strain. Microscopic inspection of the coatings suggests that the decrease in the coating resistance is a consequence of defects originated by cracks on the phosphate and by loss of adhesion at the polymer/pigment interface.

Keywords: Coil coating; Forming; Corrosion; EIS; SEM

1. Introduction

The widespread use of coil-coated steel in many fields of applications brings great relevance to the understanding of the effect of cold drawing on a coated system. It is known that mechanical deformation of organic-coated steel leads to a reduction of anti-corrosive protection properties, either due to the effects at the level of the polymer, or as a consequence of loss of adhesion at the polymer/substrate interface. Quantification of these effects on the corrosion performance, however, still lacks well-established criteria and methodologies. Evaluation of the forming limits of coil-coated steel sheets is often performed by deep drawing of cups followed by empirical determination of cracking and loss of adhesion after standard corrosion tests. However, the shapes of these cups involve a complex distribution of strain along the surface, and the degradation considered usually corresponds only to the areas with the most severe strain and the tests do not really lead to satisfactory correlations between mechanical deformation and corrosion degradation.

A deeper insight of the effect of forming can in principle be expected if the degradation is correlated with the degree of strain [1,2]. For the estimation and monitoring of the protective properties of organic-coated metals, electrochemical impedance spectroscopy (EIS) has given excellent results in many practical situations [3] and is thus, a promising technique for the study of the strain degradation effects. In a previous study, it was observed that some coatings became more prone to water absorption after they had been submitted to mechanical deformation [4], whereas, the effect of uniaxial strain on the electrochemical parameters obtained from impedance measurements has shown a good correlation between the parameters of the system: double layer capacitance, charge transfer resistance and film resistance and the elongation of the sample [5]. The aim of the present work was to extend the conclusions based upon uniaxial strain to other types of strain. With this aim, samples with uniaxial, biaxial and plane strain were studied by EIS and by scanning electron microscopy (SEM).

2. Experimental

2.1. Materials

The material used was coil-coated electrogalvanised steel, consisting of steel sheet (0.8 mm thickness) coated with a 7 μm zinc layer and an organic coating. The steel was ST14 grade (DIN 1623), with a high ductility, therefore, recommended for deep-drawing work. Before application of the

---

* Corresponding author. Tel.: +351-21-841-7234; fax: +351-21-840-4589.
E-mail address: alda.simoes@ist.utl.pt (A.M. Simões).

0013-4686/$ – see front matter © 2004 Elsevier Ltd. All rights reserved.
doi:10.1016/j.electacta.2004.03.044

organic layer, the substrate was given a pre-treatment consisting of phosphatation followed by a chromate rinse. The organic coating consisted of a 5 μm polyester primer plus a 15 μm polyurethane intercoat (both Cr-free). To achieve faster degradation, the system did not include a topcoat. Uniaxial strain was applied to panels of 30 mm × 250 mm, resulting in elongations of: 0, 9, 11, 16, 19 and 23%. The elongation ε and the true strain ϕ are given by

$$\varepsilon\,(\%) = \frac{l - l_0}{l_0} \times 100 \tag{1}$$

and

$$\phi = \ln\left(\frac{l}{l_0}\right) \tag{2}$$

where l_0 and l represent the distance between markings, before and after traction, respectively. Biaxial strain and plane strain were applied to circular samples with 20 cm diameter (Fig. 1). Five degrees of plane strain were produced, the final heights of the specimens being 15, 18, 20, 23 and 25 mm. For the biaxial strain, the increasing strain corresponded to cup heights of 18, 21, 24, 30 and 35 mm. All deformations were made at room temperature.

SEM inspection was made on samples selected among the ones above-mentioned, but also on a sample that had been uniaxially drawn until total rupture.

2.2. Electrochemical experiments

A three-electrode arrangement was used, with a saturated calomel electrode as reference, a platinum counter electrode and the working electrode consisting of the coated specimen. The sample area (3.8 cm^2) was delimited by gluing to the surface commercial polymethylmethacrylate (PMMA) tubes, which were filled with 5 wt.% NaCl aqueous solution. All measurements were performed at room temperature, under natural aeration, inside a Faraday cage. Impedance measurements were periodically made, at the open circuit potential, typically in the frequency range 50–5 mHz, with seven points per decade and with amplitude of 10 mV rms, using a Gamry FAS1 Femtostat + PC4 Controller Board. A minimum of three samples was tested for each strain, with good reproducibility. Fitting of the spectra was made with the EQUIVCRT software [6].

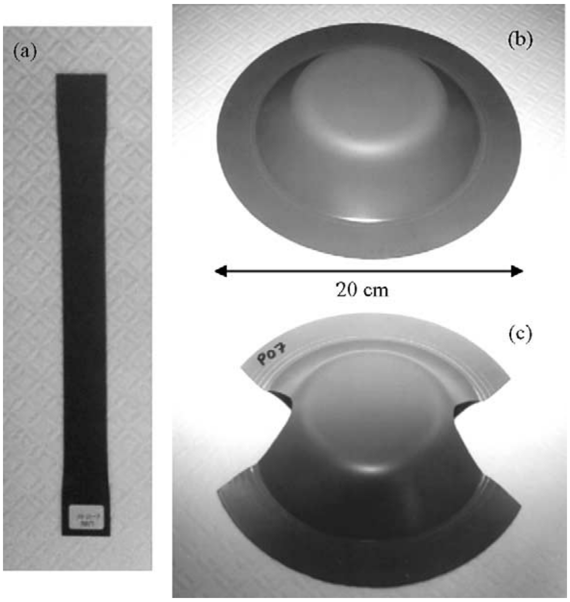

Fig. 1. Samples used in the study, with uniaxial (a), biaxial (b) and plane (c) strain.

2.3. SEM/EDS

SEM inspection of the surfaces and of cross sections was made using a Jeol JSM 6301F scanning microscope (10–15 kV) with a Noran Voyager energy dispersion spectrometer (EDS).

3. Results

3.1. EIS

The typical impedance spectra obtained on unstrained samples consisted of a capacitive response (associated with the dielectric properties of the polymer film) that lasted for several days (Fig. 2). In the example presented the response remained capacitive during the first 15 days of exposure and the film resistance was above $10^{10}\ \Omega\,\mathrm{cm}^2$. After 21 days, a significant decrease of the low frequency impedance was observed, revealing a reduction in the protective properties of

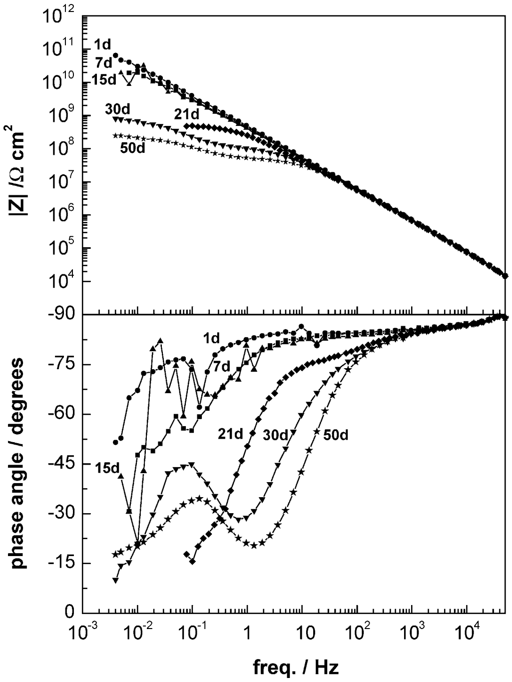

Fig. 2. EIS spectra obtained with an unstrained sample for various times of immersion (between 1 and 50 days).

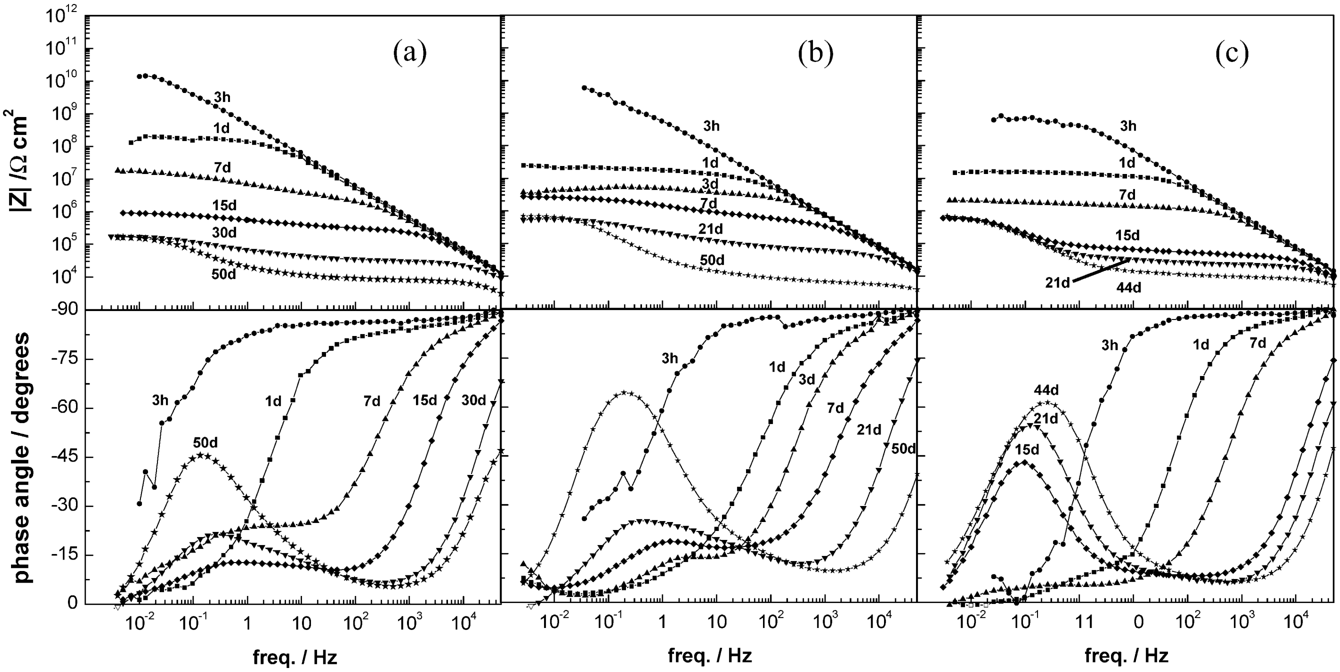

Fig. 3. EIS spectra obtained on samples with (a) 19% of uniaxial elongation; (b) plane strain (23 mm height) and (c) biaxial strain (24 mm height). Duration of the exposure expressed in the figure as hours (h) or days (d).

the coating. For longer exposure times, a second time constant appeared at the low frequencies, revealing the existence of corrosion underneath the coating. In the strained samples the general shape of the spectrum was identical, with a capacitive response in a first stage and a second time constant developing with time as the total impedance of the system decreased. It is apparent that the impedance was smaller in the strained samples from the first stages of immersion and also that it decreased more rapidly with time (Fig. 3). This process was faster in the samples with biaxial or plane strain, with respect to those with uniaxial strain. At the end of the experiment the coating resistance had reached values of approximately $10^4\ \Omega\,\mathrm{cm}^2$, revealing a highly degraded coating. Concomitantly, with this decrease in the coating resistance, the low frequency process became well developed, and blisters in the coating became well visible to the naked eye.

The spectra were numerically fitted using the equivalent circuit in Fig. 4, which is commonly used to describe a painted metal undergoing corrosion under the delaminated areas, without diffusion control. In this circuit, R_s is the uncompensated resistance between the reference and the working electrodes, R_f the film resistance, R_{ct} the charge transfer resistance, Q_f and Q_{dl} correspond to the film capacitance and the double layer capacitance, respectively (both treated as constant phase elements). The film resistance obtained from the fitting started from high impedance values, decreased abruptly in the first 10 days of immersion and then asymptotically approached a nearly constant value (Fig. 5). Q_{dl} was generally detected after a R_f drop to a value below $10^7\ \Omega\,\mathrm{cm}^2$, appearing first in the samples with higher strain, and being detected only after 1 month on the unstrained samples. For uniaxial strain, Q_{dl} showed a fast increase, particularly for higher strains and then, after 15–21 days, it also tended to a constant value. For samples with elongation of 19 and 23%, the values were similar and at the end of experiment attained values in the order of $10^{-5}\ \mathrm{F\,cm^{-2}}$. The samples with plane strain (Fig. 6) and biaxial strain (Fig. 7) showed a trend similar to the one described above, although the degradation was faster. In all the samples, the decrease in the coating resistance was accompanied by a decrease of the charge transfer resistance and an increase of the double layer capacitance, meaning that the area that had become active underneath the coating was increasing with time, as the coating gradually became less protective. This variation of the double layer capacitance and the charge transfer resistance was most abrupt in the biaxially strained samples, which very early reached Q_{dl} values in the order of $10^{-5}\ \mathrm{F\,cm^{-2}}$, values that remained nearly constant until the end of experiment. In contrast, the film resistance varied gradually with time and also with the strain. These results clearly show that the trend of the various parameters is the same in the different

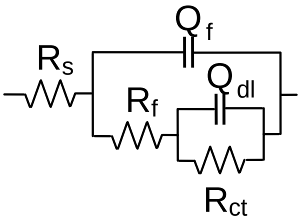

Fig. 4. Equivalent circuit used for fitting.

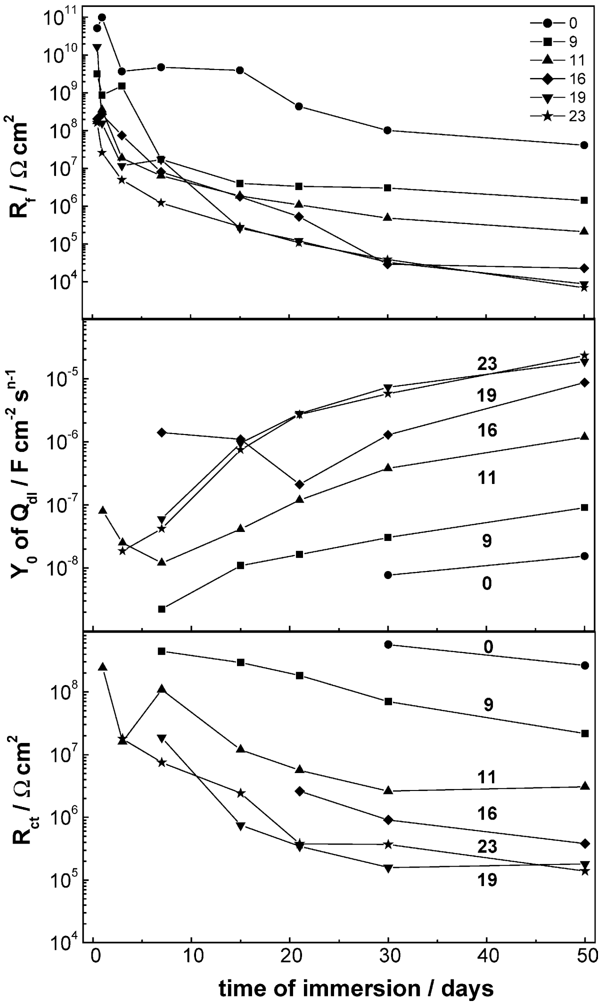

Fig. 5. Evolution of film resistance (R_f), Y_0 of Q_{dl} (double layer capacitance) and charge transfer resistance (R_{ct}) for the samples with uniaxial strain. Elongation (%) indicated in the figure.

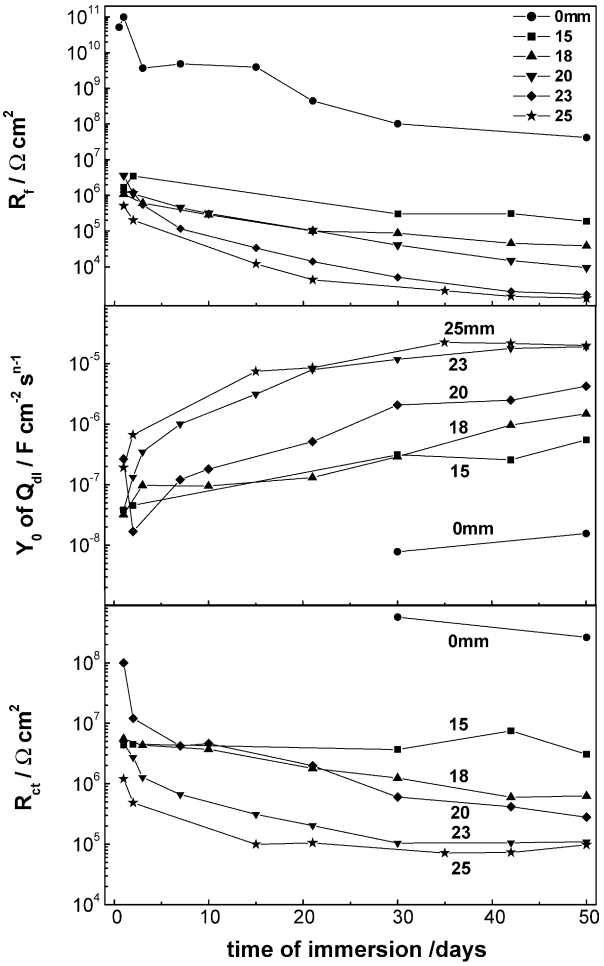

Fig. 6. Evolution of film resistance (R_f), Y_0 of Q_{dl} (double layer capacitance) and charge transfer resistance (R_{ct}) for the samples with plane strain. Cup heights of the samples (mm) indicated in the figure.

systems and they all reveal a good sensitivity to the applied strain. However, the parameters presented so far, such as the elongation or the height of the cups in the biaxial or plane strain can be used with success for comparison of samples with only one type of deformation, but not between samples with different types of mechanical action. Thus, it was decided to use an alternative parameter, the equivalent plastic strain, ϕ_v, which is a measure of the plastic deformation experienced by an object, by accounting its strain in each one of the three axis, x, y and z. It can be calculated as [7]:

$$\phi_v = \sqrt{\frac{2}{3}(\phi_x^2 + \phi_y^2 + \phi_z^2)} \tag{3}$$

where ϕ_x, ϕ_y and ϕ_z are the strains along the three orthogonal axis. Since the coating resistance was the parameter that revealed the most smooth and most regular variation, it was decided to choose it for the correlation. Fig. 8 shows the R_f evolution with ϕ_v at various instants of immersion. R_f decreases with time of immersion and, for any time, the film resistance is seen to be lower for the higher degrees of strain. The drop of the coating resistance is practically linear when caused by a small strain ($\phi_v \leq 0.15$) whereas for higher values it tends to a constant resistance value. These results also show that the samples with biaxial strain attained in practice the highest equivalent strain, which explains the severe degradation observed. The shape of the curves in the case of the biaxial strain suggests that the degradation occurs by two mechanisms, one occurring at low equivalent plastic strains and the other above a critical value, which in the case of our system seems to be around $\phi_v \leq 0.15$.

3.2. SEM

Observation of samples strained up to rupture revealed a large number of microscopic craters on the surface (Fig. 9(a)). These craters, with dimensions typically below 5 μm, were always adjacent to a solid particle. These particles were rich in elements such as Ti and Ba, (Fig. 9(b)) which confirmed that they were pigments from the coating formulation. These craters revealed loss of adhesion between the polymer and the pigments as a consequence

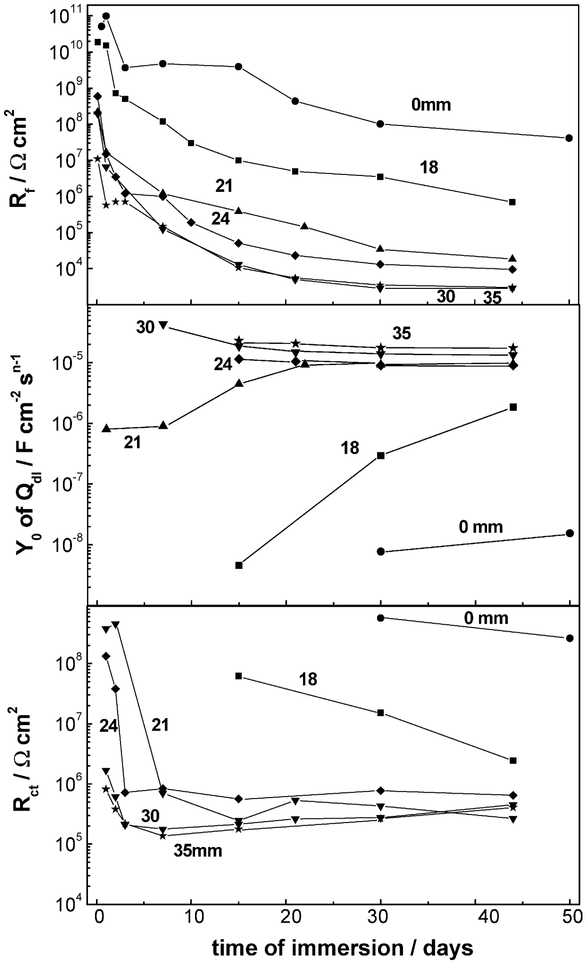

Fig. 7. Evolution of film resistance (R_f), Y_0 of Q_{dl} (double layer capacitance) and charge transfer resistance (R_{ct}) for the samples with biaxial strain. Cup heights of the samples (mm) indicated in the figure.

of the internal stresses. Although these defects could not be detected in the samples with low deformation, they also appeared as a result of immersion, provided it followed the deformation step. In fact, SEM inspection of the coating revealed a significant number of microscopic holes in samples with deformation (Fig. 10(b2) and (c2)), which can only result from the detachment of pigment particles. These holes were not present in the unstrained samples (Fig. 10(a2)).

Strain also affected the substrate. The electrodeposited zinc layer, which revealed the typical morphology of zinc crystals (Fig. 11(a)), developed, as a result of strain, a network of cracks (indicated in Fig. 11(b)). Further, the orientation of the crystals changed, becoming aligned with the direction of strain.

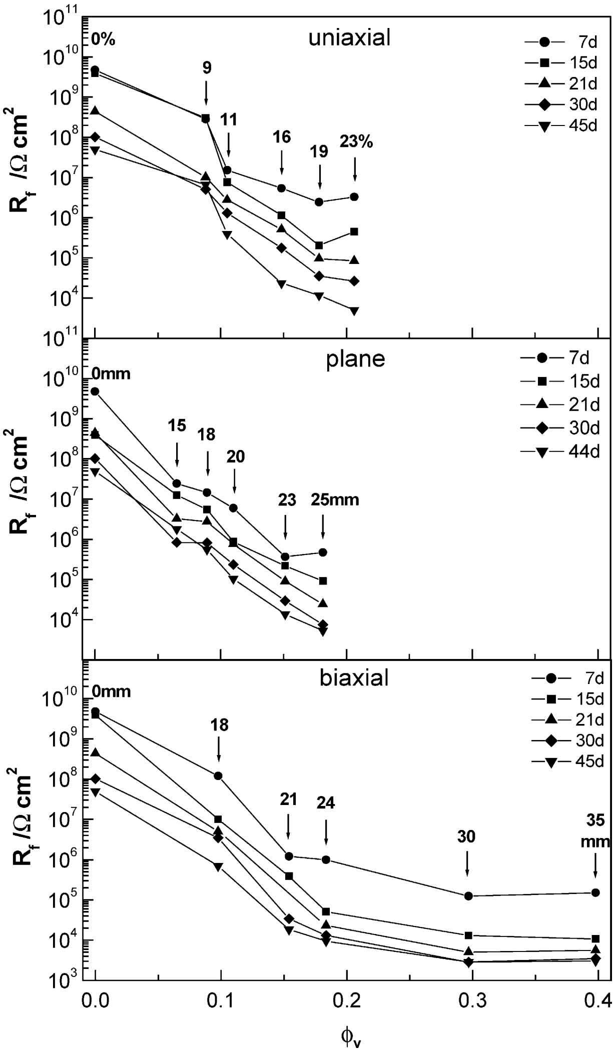

Fig. 8. Variation of the coating resistance with the equivalent plastic strain, for uniaxial (a), plane (b) and biaxial (c) strain. Time of immersion (days) indicated in the figure.

Observation of the phosphate layer in samples without organic coating, has shown the formation of cracks normal to the strain direction. These cracks increased in number and width as the elongation increased (Fig. 12). The samples with biaxial strain revealed cracking with random orientation, while total detachment of the phosphate occurred in parts of the surface (Fig. 12(d)).

Table 1
Thickness of complete system determined from SEM of cross–cut samples

	Unstrained	Uniaxial	Plane		Biaxial	
	$\phi_v = 0$	$\phi_v = 0.2$	$\phi_v = 0.07$	$\phi_v = 0.18$	$\phi_v = 0.1$	$\phi_v = 0.4$
Thickness (μm)	852 ± 5	815 ± 10	819 ± 3	766 ± 10	766 ± 12	588 ± 10
Reduction (%)	–	4.3	3.9	10.1	10.1	31.0

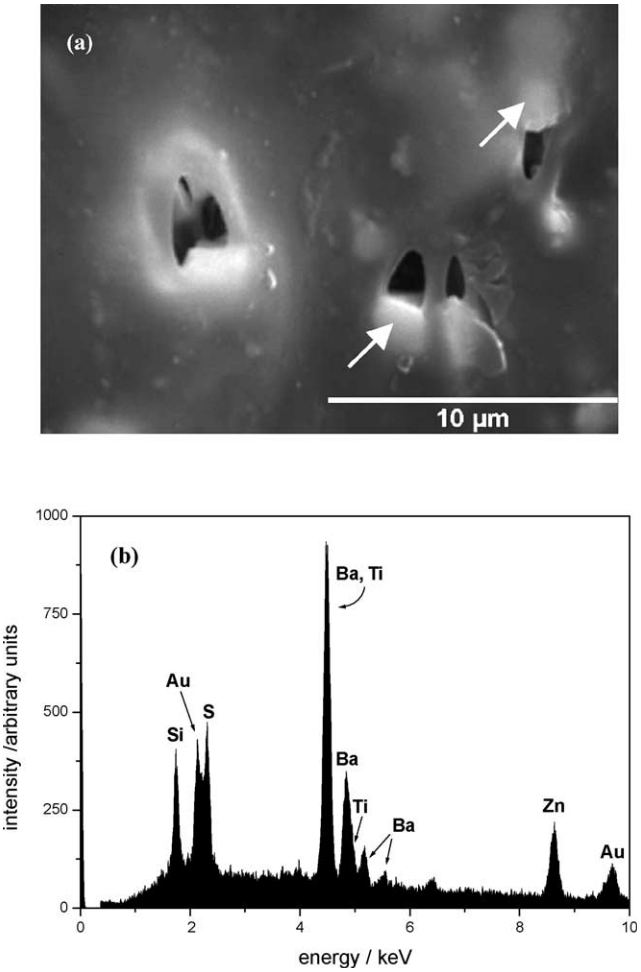

Fig. 9. (a) Micrograph of the coating surface of a sample with strain attaining rupture; inorganic particles identified with arrows; (b) EDS microanalysis of the inorganic particles. Note: the Au peaks are due to the conductive coating applied for the microscopy.

The thickness reduction caused by the strain was determined from micrographs made on cross sections and the results are presented in Table 1 for the maximum and minimum strains of the different types of deformation. Due to the large dispersion observed in the thickness of the polymer film, the measurements were made on the complete panel (steel + zinc + organic coating). The total thickness reduction was in most cases in the range 3–10%, and only reached 31% for the maximum biaxial strain.

4. Discussion

The EIS results have clearly shown that the protective properties of the coated system decrease with increasing strain and the coating resistance proved to be a sensitive parameter to the loss of protective properties of the coating. R_f is generally accepted as a measure of the barrier effect of a coating to the permeation of ions, gases and water. Q_dl and R_ct, on the other hand, are related to the area where solution contacts the metal and thus, give information on the delamination of the organic coating from the substrate. In this work, both the coating resistance and the charge transfer resistance decreased with the time of immersion and with the strain, whereas the double layer capacitance increased with both these factors. The correspondence between R_f, R_tc and Q_dl was very good and these parameters were all sensitive to the effects of strain and to the loss of protection. The correlation between the equivalent plastic strain and the coating resistance gave excellent results and allowed the comparison among the three types of strain. The plots of the film resistance versus ϕ_v gave a practically linear plot up to $\phi_\mathrm{v} \sim 0.15$, with a slope that is approximately independent of both type of strain and time of immersion. This slope is of about three orders of magnitude for an increase of ϕ_v of 0.15. This resistance decay clearly exceeds the one expectable solely from thickness reduction, assuming constant film resistivity and can be interpreted as being associated to the mechanism of film degradation caused by deformation. Consequently, the slope should in principle decrease with temperature (particularly if the glass transition temperature is crossed) and more generally with ductility of the polymer.

The shape of the R_f versus equivalent plastic strain reveals a process occurring in two stages. According to the literature, cold-drawing of ductile polymers under uniaxial stress also occurs in two phases, the first consisting of plastic yielding deformation at a local maximum, followed by necking and finally to some strain hardening [8]. Further, under certain limits of drawing, strain can even enhance the properties of polymers in the drawing direction, due to the hardening process [9]. In the complex case of polymer films including inorganic particles in its matrix, the presence of pigments significantly affects the stress–strain behaviour of the coating. Thus, it can be envisaged that at low strain some relaxation and rupture of polymer chains as well as some movements on the pigment particles occurs. Morphologically, this can be observed in terms of roughness or curling [5]. Water penetration due to immersion of the samples may then lead to expanding forces at polymer/pigment interface, with consequent weakening of the adhesion forces between the polymer matrix and the pigment. The interface between pigments and polymers is often considered to constitute preferential paths for water diffusion. With the effects induced by deformation, diffusion becomes easier either because of the voids formed or, at low strain, by the residual stresses at the interface.

The observed cracking and localised de-adhesion of the phosphate layer also increased with strain. While this was shown for uncoated phosphated samples, this kind of processes can be expected also underneath the organic coating. As a consequence, zinc is left uncovered from the beginning of the exposure, leaving preferential sites for metal/solution contact as soon as the solution crosses the coating and reaches the metal surface. Naturally, the relevance of these effects is to a large extent a function of the barrier properties, the type of polymer and the pigmentation.

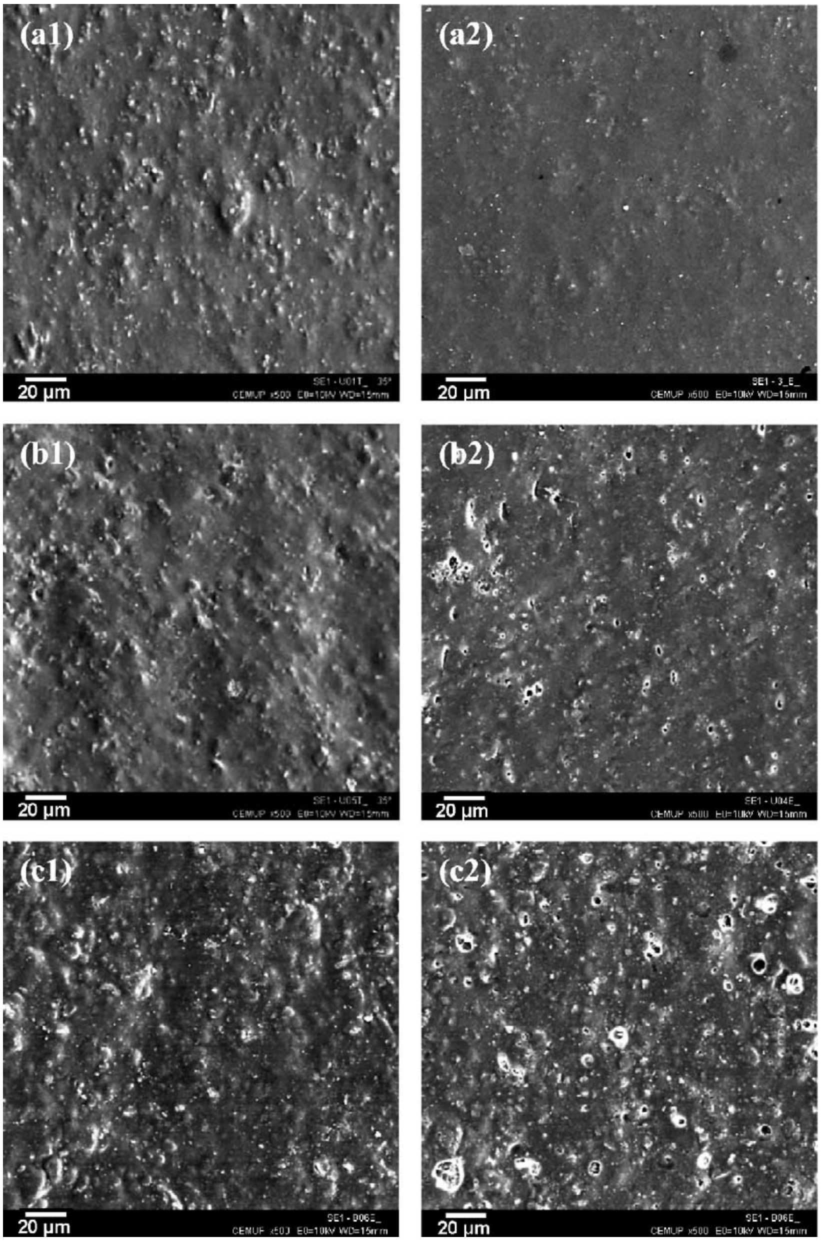

Fig. 10. Micrographs of the paint surface prior to and after 3 months of immersion: unstrained sample before (a1) and after (a2) immersion; sample with 23% of elongation before (b1) and after (b2) immersion; sample biaxially strained—cup height 35 mm—before (c1) and after (c2) immersion.

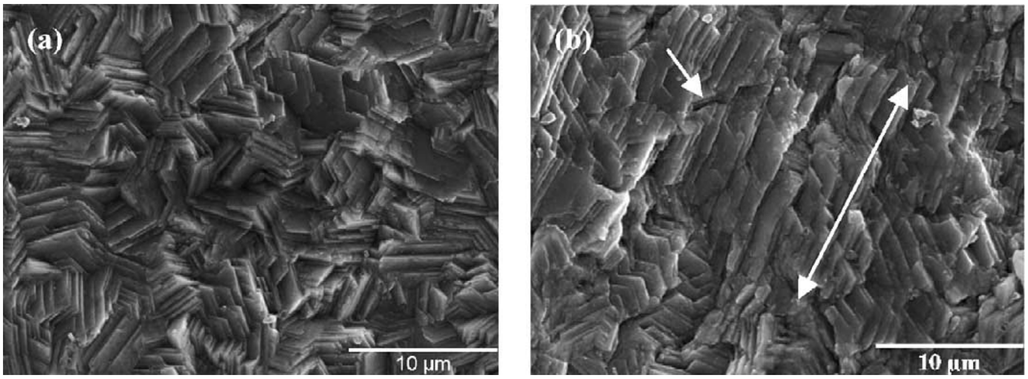

Fig. 11. Micrographs of the surface of electrodeposited zinc on samples without strain (a) and with uniaxial ($\epsilon = 23\%$) strain; strain direction as indicated.

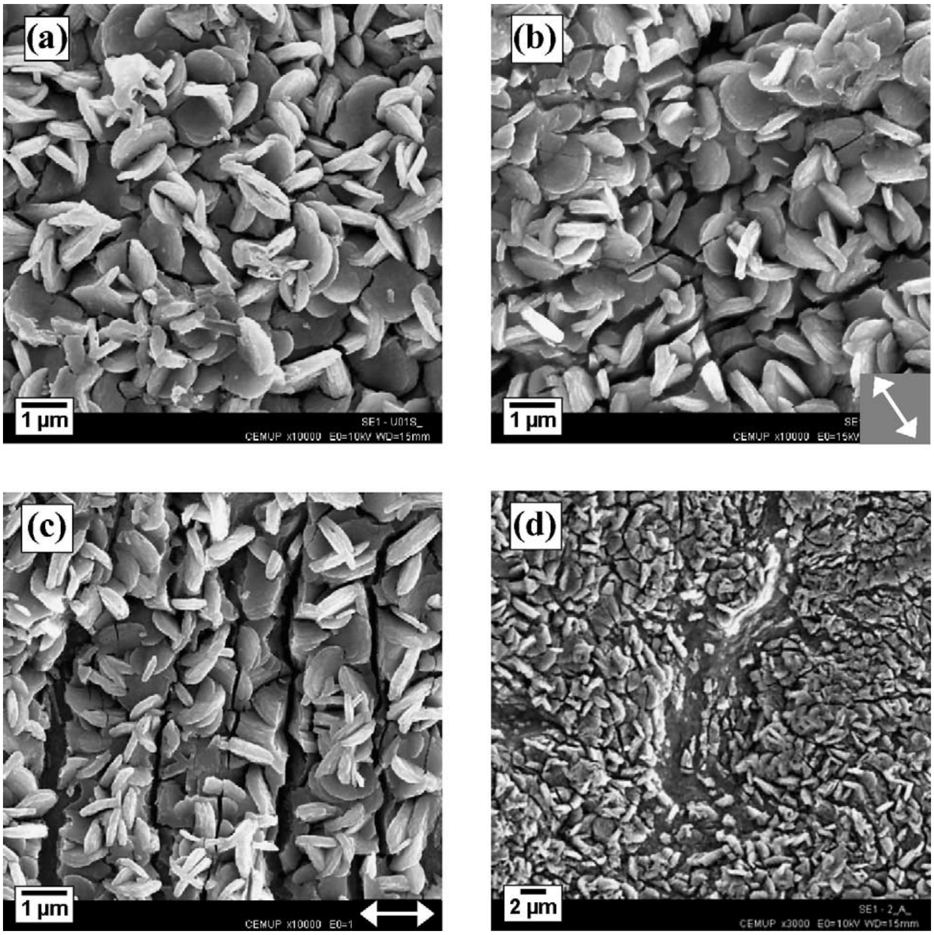

Fig. 12. Micrographs of the phosphate layer for: uniaxially strained samples with elongation of 0% (a), 11% (b) and 23% (c) and for a biaxially strained sample with cup height of 35 mm (d). Direction of elongation indicated by an arrow in micrographs (b) and (d).

The effects of plastic deformation can thus, be described at several levels, as schematically described in Fig. 13:

(a) re-orientation of the zinc crystals;
(b) cracking of the phosphate layer, with consequent loss of adhesion of the coating at the cracks;
(c) drop of adhesion forces at the polymer/pigment interface.

This last phenomenon leads not only to the formation of voids inside the matrix, but also a global reduction in the effective length that the water needs to cross before reaching the substrate, thus, accelerating permeation and corrosion.

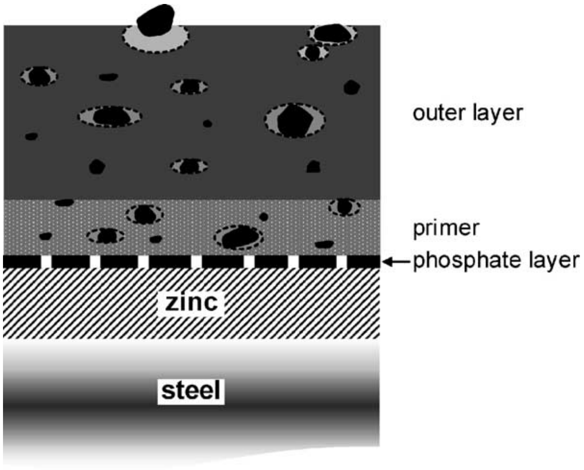

Fig. 13. Diagram showing the effects of the strain on the coated system.

5. Conclusions

EIS and SEM were used to achieve valuable information regarding the effect of uniaxial, biaxial and plane strain on the corrosion protection given by coil coatings. The protective properties were assessed by electrochemical parameters obtained from the EIS measurements. These parameters were sensitive to the induced strain: the film resistance and the charge transfer resistance decreased whereas the double layer capacitance increased with increasing strain. Based on the microscopic inspection of the coating films it was concluded that strain creates defects originated by loss of adhesion between the polymer and the pigments.

The zinc layer was also stressed and cracks on the phosphate layer left areas of metal uncovered by the inorganic layer.

For low plastic strain, the coating resistance decreased logarithmically with the equivalent plastic strain with an approximately constant slope, which was practically constant with time and independent of the type of deformation. This resistance decay was caused mostly by the physical damaging of the coating during forming work and not by thickness reduction. For higher strain, the changes in the coating resistance were much smaller and ultimately lead to the loss of adhesion to the pigment particles.

Acknowledgements

The authors acknowledge funding from the ECSC programme (contract no. 7210-PD-189) and the support from POCTI. DOC/ThyssenKrupp is also acknowledged for preparation and forming of the samples. A very special acknowledgement to Dr. Michael Rohwerder for many useful discussions.

References

[1] F. Deflorian, L. Fedrizzi, S. Rossi, Corros. Sci. 42 (2000) 1283.
[2] V. Lavaert, P. Praet, M. Moors, E. Wettinck, B. Verhegghe, Prog. Org. Coat. 39 (2000) 157.
[3] G. Grundmeier, A. Simões, Corrosion protection by organic coatings, in: M. Stratmann, G.S. Frankel (Eds.), Encyclopedia of Electrochemistry, Corrosion and Oxide Films, vol.4, Wiley-VCH, Weinheim, 2003.
[4] A.S. Castela, A.M.P. Simões, M.G.S. Ferreira, Effect of ageing on the formability of coil coatings, in: P.L. Bonora, F. Deflorian (Eds.), Electrochemical Methods in Corrosion Research VI, Trans Tech Publications, 1998.
[5] A.C. Bastos, A.M. Simões, Prog. Org. Coatings 46 (2003) 220.
[6] B.A. Boukamp, Solid State Ionics 18–19 (1986) 136;
B.A. Boukamp, Solid State Ionics 20 (1986) 31.
[7] I.M. Ward, W. Hadley, An Introduction to the Mechanical Properties of Solid Polymers, Wiley, New York, 1993.
[8] Z. Xixiong, J. Polym. Sci. B: Polym. Phys. 31 (1993) 1667.
[9] I. Karacan, D.I. Bower, I.M. Ward, Polymer 35 (1994) 3411.